Received: 11 July 2020 | Accepted: 16 December 2020

DOI: 10.1111/jvim.16020

CASE REPORT

Journal of Veterinary Internal Medicine Open Access

ACVIM American College of Veterinary Internal Medicine

Cerebrospinal fluid flow on time-spatial labeling inversion pulse images before and after treatment of congenital hydrocephalus in a dog

Daisuke Ito[1] | Chieko Ishikawa[1] | Nick D. Jeffery[2] | Masato Kitagawa[1]

[1]Laboratory of Veterinary Neurology, Department of Veterinary Medicine, College of Bioresource, Nihon University, Kanagawa, Japan

[2]Veterinary Medicine and Biomedical Science, Department of Small Animal Clinical Sciences, Texas A&M University, Texas

Correspondence
Daisuke Ito, Laboratory of Veterinary Neurology, Department of Veterinary Medicine, College of Bioresource, Nihon University, Kanagawa, Japan.
Email: itou.daisuke@nihon-u.ac.jp

Abstract

A 3-month-old male cross-breed dog presented with signs of progressive diffuse brain disease. Noncommunicating congenital hydrocephalus concurrent with cervical syringomyelia was diagnosed on magnetic resonance images. On time-spatial labeling inversion pulse (Time-SLIP) images CSF flow through the mesencephalic aqueduct was poorly defined and there was flow into the syrinx across the craniocervical junction. After percutaneous ventricular drainage and ventriculoperitoneal shunting, CSF flow through the aqueduct was clearly detected and flow into the syrinx disappeared. In addition, CSF flow in the subarachnoid space at the pons and ventral aspect of the cervical subarachnoid space was restored. Signs of neurological dysfunction improved after ventriculoperitoneal shunting and the cerebral parenchyma was increased in thickness on 2-year follow-up computed tomography images. Patterns of CSF flow on Time-SLIP images before and after CSF drainage or ventriculoperitoneal shunting aid in clarifying disease pathogenesis and confirm effects of CSF drainage.

KEYWORDS
CSF, hydromyelia, magnetic resonance imaging, syringomyelia, Time-SLIP

1 | INTRODUCTION

In dogs, internal hydrocephalus is defined as excessive accumulation of cerebrospinal fluid (CSF) within the ventricular system.[1] The causes of congenital internal hydrocephalus are suspected to be interruption or obstruction of CSF circulation (noncommunicating), or dysfunction of CSF absorption (communicating),[1,2] although the precise pathogenesis in each individual case often remains unknown. Ventricular peritoneal shunting (VPS) is the gold standard to treat congenital hydrocephalus in animals[3-7] and reduced postoperative ventricular size accompanied by increased brain parenchyma volume correlate with improvement of clinical signs.[7] Although VPS can improve clinical status,[3-6] a methodical approach to standardize decision making is required because of the variable outcome after VPS[4,7] and the risk of complications, including shunt obstruction, pain, infection, and excessive drainage.[8]

In human medicine, the CSF-tap test (CSF-TT) (ie, drainage) is used to predict the efficacy of surgical treatment in both congenital and acquired hydrocephalus.[9-17] However, a recent systematic review on reliability of CSF-TT in idiopathic normal pressure hydrocephalus (iNPH) demonstrated that a negative response to CSF-TT does not necessarily imply ineligibility for shunting.[18] Recently, CSF dynamics

Abbreviations: CCJ, craniocervical junction; CSF, cerebrospinal fluid; CSF-TT, CSF-tap test; CT, computed tomography; IVP, intraventricular pressure; MRI, magnetic resonance imaging; T1W and T2W, T1 and T2 weighted; Time-SLIP, time-spatial labeling inversion pulse; VPS, ventricular peritoneal shunting.

have been evaluated using the time-spatial labeling inversion pulse (Time-SLIP) sequence—a magnetic resonance imaging (MRI) technique that defines CSF dynamics during short imaging periods (~6 seconds).[19-23] In human diseases that disturb normal CSF flow, such as iNPH, or congenital and acquired hydrocephalus, CSF flow is difficult to observe in the ventricular system, including the interventricular foramen (foramen of Monro), 3rd ventricle or mesencephalic aqueduct on Time-SLIP images.[19-21,23] In addition, in patients with intracranial arachnoid diverticulum in the middle fossa, CSF flow is not detected between the basal cistern and diverticulum.[20] In those patients, Time-SLIP can confirm whether surgical treatment successfully restores CSF flow in the ventricular system or in the vicinity of the lesion.[19-21,23] Furthermore, patients with restoration of CSF flow on postsurgical Time-SLIP images are reported to have a good prognosis.[19-21] In veterinary medicine, Time-SLIP imaging is rarely used; there is only a single case report describing CSF flow in the aqueduct of a dog with obstructing hydrocephalus due to brain tumor.[24]

In this report, we describe CSF flow at the aqueduct and craniocervical junction (CCJ) on Time-SLIP images obtained before and after VPS in a dog with congenital hydrocephalus and syringomyelia.

2 | CASE HISTORIES

A 3-month-old, 1.48 kg, male cross-breed (Maltese × toy poodle) dog was referred to our hospital with a 1-month history of signs of progressive diffuse brain lesion including altered mental status, circling to the left, ataxia, left head tilt, nystagmus, and hyperesthesia when handling the head. Medical treatment using prednisone (0.5 mg/kg, Q12h) at the referring veterinary clinic ameliorated the clinical signs for short periods but the poor mental status, poor appetite, and severe signs of vestibular disease recurred.

At presentation, the dog was in lateral recumbency and somnolent with a whole-body tremor. The dog was generally settled but showed episodic aggression and confusion. The head was enlarged and dome shaped, and there was ventrolateral strabismus, left head turn, and scoliosis. Open calvarial sutures and persistent fontanelles were detected by palpation. Neurological examination revealed postural reaction deficits in all limbs, bilateral deficits in menace responses and positional strabismus in the left eye, nystagmus with slow phase to the left and left head tilt. Spinal reflexes were intact in all limbs. Judging from these tests, neurological localization was thought to be the brain (forebrain, brain stem, and cerebellum) and, also, because of the scoliosis, likely a lesion affecting the cervical spinal cord. Persistent suture lines and fontanelles and thinning of the calvaria were detected on head radiographies, and scoliosis was apparent on a dorsoventral view of the cervical vertebral column. Ultrasonography of the head revealed extremely dilated lateral ventricles and the ventricle: brain ratio[25] was approximately 95%. Congenital hydrocephalus and presumptive concomitant syringomyelia were tentatively diagnosed.

2.1 | Conventional MRI findings

Magnetic resonance imaging was performed using a 1.5-T superconducting unit (EXCELART Vantage, Canon Medical Systems Corporation, Tochigi, Japan), with the dog under general anesthesia and in sternal recumbency. On mid-sagittal T2-weighted (W) images, the entire ventricular system was extremely dilated, there was an supracollicular fluid accumulation in the quadrigeminal cistern and cervical syringomyelia (Figure 1A). There was no CSF signal in the subarachnoid space surrounding the brain and spinal cord on T2W images (Figure 1A,B). No abnormal signal intensity was detected in the brain parenchyma on T1W, T2W, fluid attenuated inversion recovery, and postcontrast T1W images.

2.2 | Time-SLIP sequence

Use of the Time-SLIP sequence (and CSF-TT) was approved by the hospital ethical committee (an approval number was not allocated), and written informed consent was obtained from the owner.

After conventional MRI sequences, Time-SLIP images were obtained at 2 sites: (a) the mesencephalic aqueduct (the tag was set perpendicular to the aqueduct) to evaluate CSF flow in the aqueduct and subarachnoid space ventral to the brain stem (a region equivalent to the prepontine cistern in humans and, below, this CSF space is described as the "prepontine cistern") and (b) the CCJ (the tag was set perpendicular to the ventral aspect of the cervical spinal cord at C1 vertebra) to evaluate the flow in the cervical subarachnoid space and the flow into the syrinx before and after CSF-TT and VPS. The parameters of Time-SLIP images were: repetition time, 9600 milliseconds; echo time, 80 milliseconds; field-of-view, 13 × 13 cm; matrix, 160 × 192; slice thickness, 4 mm; labeled pulse (tag) width, 10 mm. Inversion time was increased in 30 increments of 50 milliseconds, starting at 1500 milliseconds. The total acquisition time was ~4.5 minutes for each sequence. If bright signal (tagged CSF) was visible in the nontagged dark CSF space, or dark signal (nontagged CSF) was visible in the tagged bright CSF space at least once, CSF was defined as "flowing" at those sites (see Appendix for description of the principle of the Time-SLIP sequence).

2.3 | CSF flow evaluation on Time-SLIP images before and after CSF-TT (drainage)

Before CSF-TT, CSF flow in the aqueduct was poorly defined (Video S1) and the flow into the syrinx at the CCJ was observed (Figure 2A-D, Video S2) and CSF flow in other areas was not detected. CSF was then percutaneously drained from the left lateral ventricle via the rostral fontanelle (CSF-TT) with the dog in sternal recumbency. Hair was shaved over the parietal area and the skin aseptically prepared using povidone-iodine and 70% ethanol. Two extension 20-cm tubes were attached to a 30-G needle inserted into

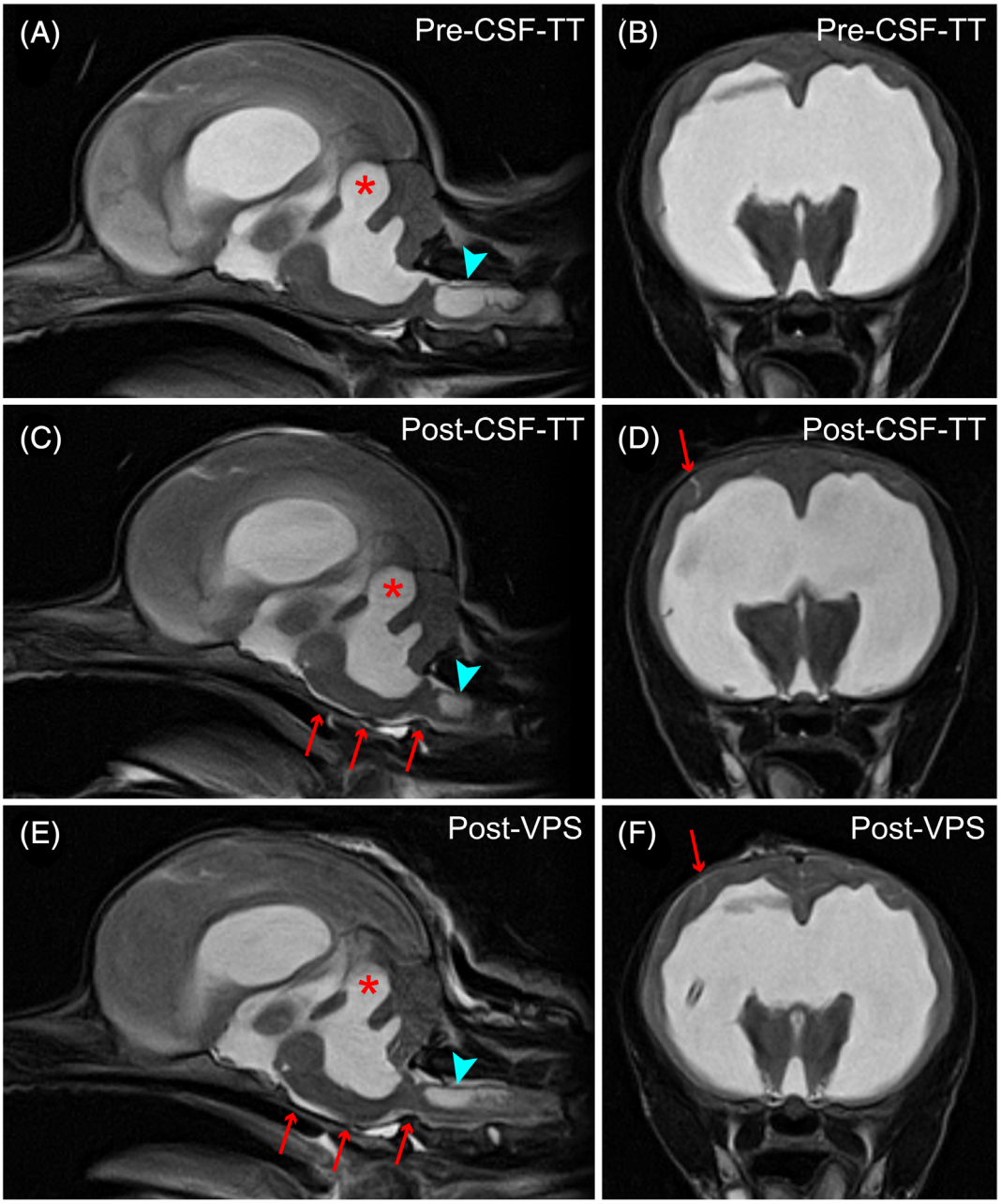

FIGURE 1 Sagittal and transverse T2-weighted (T2W) magnetic resonance (MR) images before the cerebrospinal fluid (CSF) tap test (TT), A,B, after CSF-TT, C,D, and after ventriculoperitoneal shunting (VPS), E,F. Before CSF-TT, the ventricles are extremely dilated with supracollicular fluid accumulation (asterisk) and cervical syringomyelia (blue arrow head). There was no CSF signal in the subarachnoid space surrounding the brain and spinal cord. After CSF-TT, CSF signal in the subarachnoid space was restored (red arrows). Post-VPS T2W images revealed visible reduction ventricular size, supracollicular fluid accumulation (asterisk) and syrinx (blue arrowhead), and reappearance of CSF signal in the subarachnoid space (red arrows)

the lateral ventricle and used to measure intraventricular pressure (IVP). The IVP was 32 cm H_2O (approximately 23.54 mm Hg, reference range: 8-12 mm Hg[26]), and 0.75 mL of CSF was collected (drained). Subsequent to CSF-TT, sagittal and transverse T2W, and Time-SLIP images were repeated. On T2W images, CSF signal in the subarachnoid space and cerebral sulci was restored (Figure 1C,D). On Time-SLIP images, CSF flow in the mesencephalic aqueduct was more clearly apparent compared to that observed before drainage, but flow in the prepontine cistern remained minimal (Figure 3A-D, Video S3). Flow in the ventral cervical subarachnoid space was apparent and there was no flow into the syrinx at the CCJ (Video S4).

2.4 | CSF flow evaluation on Time-SLIP images before and after VPS

During the 1st week after CSF-TT, the dog did not show any clinical improvement despite continuing medical treatment, and the owner

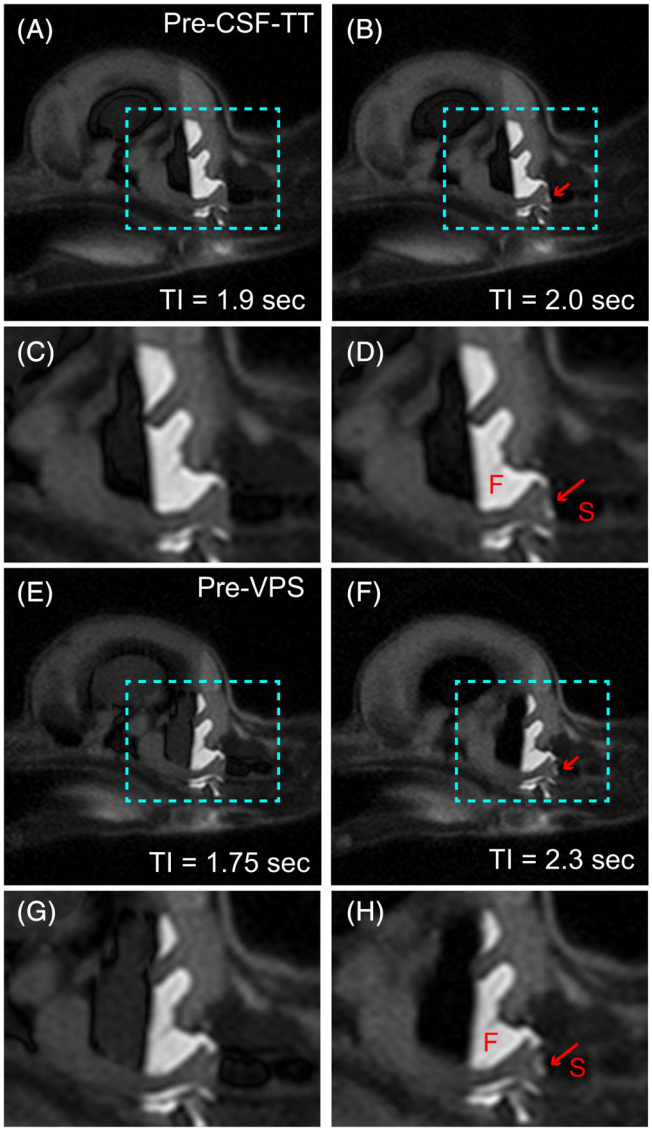

FIGURE 2 Sequential series of Time-spatial labeling inversion pulse (Time-SLIP) images at the craniocervical junction (CCJ) before the CSF tap test (CSF-TT) (A-D: C and D are enlarged images from cropped area in A and B, respectively) and ventriculoperitoneal shunting (VPS) (E-H: G and H are enlarged images from cropped area in E and F, respectively). CSF flow into the syrinx [hyperintense signal at nontagged area of the syrinx (dark background): arrows on B, D, F, and H] was detected on the images, but not in earlier parts of the sequence (A, C, E, G) (Videos S2 and S6). F, 4th ventricle; S, syrinx; TI, inversion time

opted for surgical treatment. Time-SLIP images obtained before VPS revealed no CSF flow in the aqueduct and flow into the syrinx was detected similarly to that noted before CSF-TT (Figure 2E-H, Videos S5 and S6). There was no CSF flow in the intracranial and cervical arachnoid space. A high-pressure valve ventriculoperitoneal shunt (CSF flow control valve ultrasmall, Medtronic Japan, Tokyo, Japan) was placed because intraoperative IVP was approximately 35 cm H_2O (~25.75 mm Hg). On postoperative MRI the ventricles, supracollicular fluid accumulation and syrinx were all reduced in volume and CSF signal reappeared in the subarachnoid space and cerebral sulci on T2W images (Figure 1E,F). Rostral and caudal direction of CSF flow in the 3rd ventricle and the aqueduct were apparent in addition to flow in the subarachnoid space at the prepontine cistern on Time-SLIP images tagged at level of the aqueduct (Figure 3E-H, Video S7). On Time-SLIP images at the CCJ, flow into the syrinx was not observed, instead, CSF was observed to flow in the ventral cervical subarachnoid space (Video S8).

2.5 | Clinical outcome and follow-up computed tomography findings

Two days after surgery, the mental status and appetite had improved. There were residual vestibular signs including head tilt, strabismus and ataxia, but the dog became independently ambulatory at 2 weeks after surgery. Although ataxia and learning disability persist 2 years after surgery, the dog has improved quality of life with independent walking and eating. Follow-up computed tomography (CT) scan 2 years after surgery was performed without anesthesia using a 320-slice scanner (Aquilion ONE, Canon Medical Systems Corporation, Tochigi, Japan) revealing an expanded cerebral parenchyma but persistent dilation of the 4th ventricle (Figure 4).

3 | DISCUSSION

Here we demonstrate CSF flow in the mesencephalic aqueduct and CCJ in a dog with congenital hydrocephalus and cervical syringomyelia by using Time-SLIP MRI. The patterns of CSF flow on the images before and after CSF-TT and VPS in addition to findings on conventional MRI clarify the pathogenesis and confirm effects of CSF drainage.

It has proven difficult to determine the precise patterns of CSF flow through and around the brain and CCJ in both humans and dogs. Until recently, the predominant theory ("bulk flow") posited that in normal individuals CSF was produced in the choroid plexuses and then moved, in general from rostral to caudal, through the ventricles and out through the foramina to bathe the external surfaces of the brain and then was absorbed predominantly through the arachnoid villi.[27] Since then there has been a wider adoption of the notion that "CSF is formed everywhere and resorbed everywhere"[27] and modern methods of tracking CSF flow—such as the Time-SLIP technique described here—suggest, rather, that flow is pulsatile.[28,29] This to-and-fro movement in healthy humans and animals is generated by respiratory motion (inhalation versus exhalation) and cardiac pulsation (systole versus diastole).[22,23,30-32] CSF flows rostrally during inspiration and caudally during expiration: increased blood flow into the brain is associated with increased CSF flow out of head and, similarly, during periods of decreased venous drainage there is increased CSF flow out of head.[30,31] This oscillating pattern of CSF flow occurs in coordination with respiratory and cardiac cycles on Time-SLIP images and real-time MRI in humans.[22,23,32]

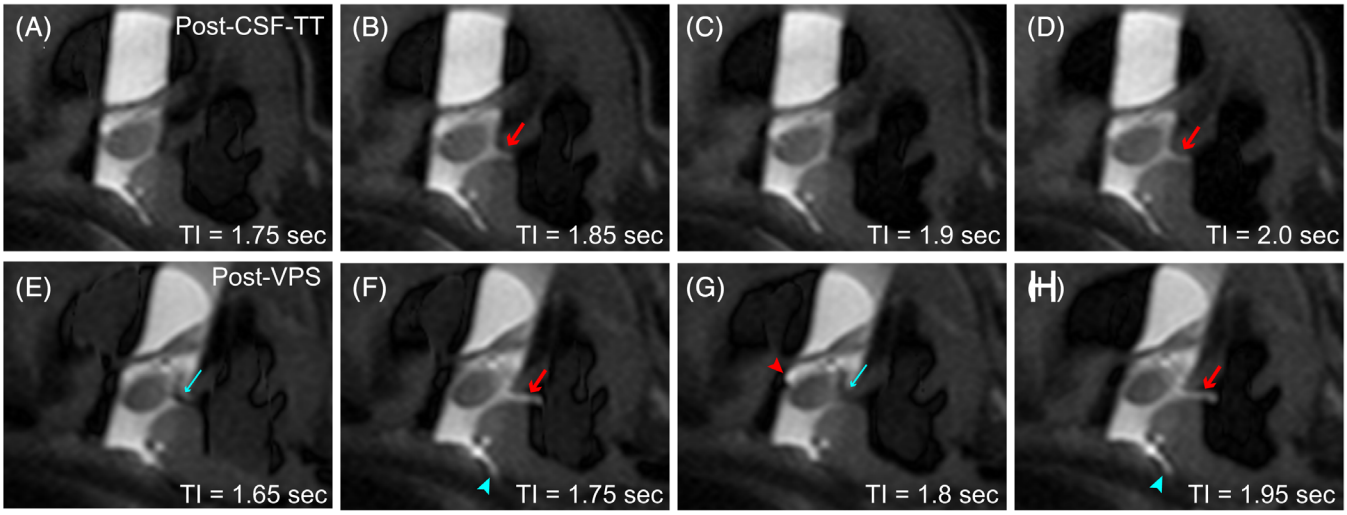

FIGURE 3 Sequential series of Time-spatial labeling inversion pulse (Time-SLIP) images at the mesencephalic aqueduct after CSF tap test (CSF-TT), A-D, and ventriculoperitoneal shunting (VPS), E-H. The tagged CSF (hyperintense signal of CSF) flow thorough the nontagged aqueduct (dark background) is apparent on the images (arrows in B, D, F, and H) (Videos S3 and S7). On the Time-SLIP images after VPS, retrograde CSF flow is detected in the 3rd ventricle, denoted by the high signal CSF from the rostral edge of the tagged area of the 3rd ventricle into the nontagged area of the ventricle where the CSF signal is dark (arrowhead in G), or by nontagged CSF (dark) signal in the caudal edge of the tagged area of the 3rd ventricle where CSF signal is hyperintense (blue arrows in E and G) (Video S7). In addition, CSF flow is detected at the arachnoid space of the pons (the prepontine cistern), recognized by tagged CSF (high CSF signal) in the nontagged (dark) area of the the prepontine cistern (blue arrowheads in F and H), which was not detected before VPS (Videos S5 and S7). TI, inversion time

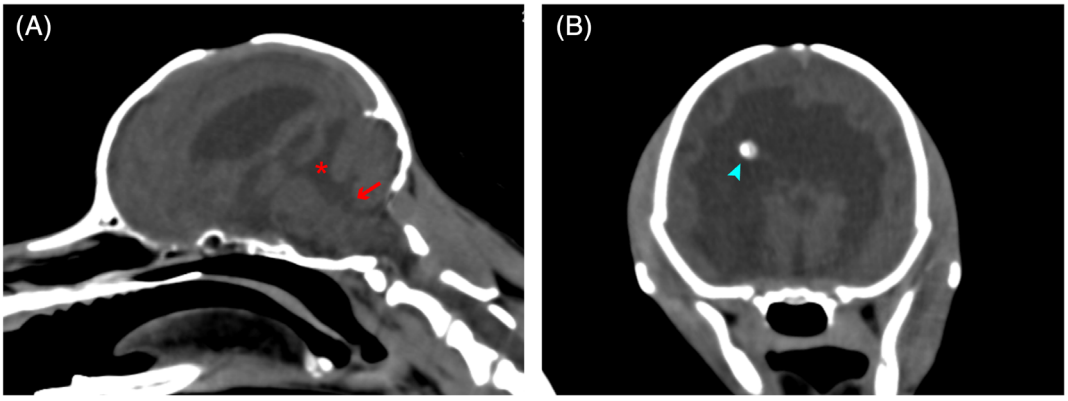

FIGURE 4 Multiplanar reconstruction images of follow-up computed tomography (CT; A, sagittal; B, transverse). The supracollicular fluid accumulation (A, asterisk) and dilation of the 4th ventricle (A, arrow) are apparent, but the cerebral parenchyma is expanded. The shunt tube is visible on the transverse image (B, blue arrowhead)

In disease states, the pattern of CSF flow is modulated by abnormal distribution of regions of high and low pressure, with flow inevitably occurring from areas of high pressure to areas of low pressure, although these regions might also continuously vary with phase of heartbeat and respiration. In small animals, intracranial "compliance" (the ability to accommodate increased volume without increase in pressure) is also considered to influence CSF dynamics and abnormal compliance may constitute a cause of hydrocephalus, especially in brachycephalic dogs.[33-35] In normal dogs, expansion of the intracranial arteries during systole compresses the intracranial CSF cistern and ventricles and also promotes flow of blood, CSF, or both, into the draining veins. In some dogs with communicating hydrocephalus, persistent high pressure cannot be detected within the ventricular system,[33-35] suggesting that CSF accumulation in the ventricles might arise because of a reduction in compliance, in which return of CSF and blood to the draining veins is impaired, perhaps because of changes in pressure, or dimension, of the epidural veins, and strong arterial pulsations in the choroid arteries and plexus exacerbate the tissue disruption caused by intraparenchymal fluid accumulation.

In our case, there was demonstrably high pressure within the lateral ventricles, implying that the normal caudal to rostral component of oscillatory flow was impeded. However, as we show using Time-SLIP, there was poor flow in both directions in the prepontine cistern and the mesencephalic aqueduct, suggesting that before intervention

there must have been high-pressure regions both rostrally and caudally, possibly due to reduced brain compliance and impaired CSF flow. Time-SLIP images obtained after CSF drainage by CSF-TT or VPS suggested that the driving forces generated by respiratory movement and heartbeat were restored, allowing normal cranial and caudal CSF flow in the aqueduct and prepontine cistern, similar to that occurring in human patients.[19] There was also impedance of flow in the cranial cervical epidural space, perhaps because of local occlusion associated with foramen magnum herniation (secondary to raised pressure in the lateral ventricles) and reduced craniospinal compliance.[36] In our case, when this subarachnoid route was blocked—before shunting—CSF was observed to flow instead into the central canal of the cord, providing an explanation for development of syringomyelia. Before CSF drainage, CSF flow into the syrinx was observed at the CCJ but, after treatment, CSF flow was apparent in the ventral cervical spinal subarachnoid space, along with decreased size of the 4th ventricle and syrinx on MRI, including Time-SLIP images. Reduction in pressure in the rostral part of the cranial cavity restored the normal dynamics of CSF movement more caudally. A similar pathogenesis of syrinx development, called the "water hammer effect," has been suggested in human syringomyelia associated with Chiari type I malformation[37-39] and dogs with syringomyelia associated with Chiari-like malformation.[40,41] There is restoration of CSF flow in the ventral cervical spinal subarachnoid space on Time-SLIP images after surgical treatment in human patients.[23]

In human medicine, CSF drainage ("CSF-TT") is used to predict the efficacy of surgical treatment in both congenital and acquired hydrocephalus patients.[9-17] If the clinical signs improved after lumbar CSF-TT in iNPH patients, or after external ventricular drainage in congenital or acquired hydrocephalus patients, the CSF-TT was judged *Positive*. In those positive patients, surgical treatments reducing CSF volume would be expected to be effective. However, a recent systematic review on reliability of CSF-TT in iNPH suggested that a negative response to CSF-TT does not necessarily make these patients ineligible for shunting, and concludes that CSF-TT has low sensitivity.[18] Restoration of CSF flow on Time-SLIP images after surgery predicts successful treatment and good clinical outcome in human patients with CSF flow diseases, including iNPH, congenital, and acquired hydrocephalus and intracranial arachnoid cyst.[19-21,23] In our case, long-term follow-up revealed good clinical outcome with expanded cerebral parenchyma on CT images, although CSF-TT before VPS was judged to be *Negative*.

We conclude that Time-SLIP images allow better definition of CSF dynamics in dogs and will lead to improved diagnostic accuracy and, therefore, a better match of treatment to pathogenesis.

ACKNOWLEDGMENT

No funding was received for this study.

CONFLICT OF INTEREST DECLARATION

Authors declare no conflict of interest.

OFF-LABEL ANTIMICROBIAL DECLARATION

Authors declare no off-label use of antimicrobials.

INSTITUTIONAL ANIMAL CARE AND USE COMMITTEE (IACUC) OR OTHER APPROVAL DECLARATION

Approved by the Animal Medical Center Management and Ethics Committee.

HUMAN ETHICS APPROVAL DECLARATION

Authors declare human ethics approval was not needed for this study.

ORCID

Daisuke Ito https://orcid.org/0000-0002-3671-1889

REFERENCES

1. de Lahunta A. Cerebrospinal fluid and hydrocephalus. In: de Lahunta A, Glass E, Kent M, eds. *Veterinary Neuroanatomy and Clinical Neurology*. 4th ed. Saunders: Toronto, ON; 2015:78-101.
2. Selby LA, Hayes HM, Becker SV. Epizootiologic features of canine hydrocephalus. *Am J Vet Res*. 1979;40:411-413.
3. Harrington ML, Bagley RS, Moore MP. Hydrocephalus. *Vet Clin North Am Small Anim Pract*. 1996;26:843-856.
4. Biel M, Kramer M, Forterre F, et al. Outcome of ventriculoperitoneal shunt implantation for treatment of congenital internal hydrocephalus in dogs and cats: 36 cases (2001-2009). *J Am Vet Med Assoc*. 2013;242:948-958. https://doi.org/10.2460/javma.242.7.948.
5. Shihab N, Davies E, Kenny PJ, Loderstedt S, Volk HA. Treatment of hydrocephalus with ventriculoperitoneal shunting in twelve dogs. *Vet Surg*. 2011;40:477-484.
6. de Stefani A, de Risio L, Platt SR, Matiasek L, Lujan-Feliu-Pascual A, Garosi LS. Surgical technique, postoperative complications and outcome in 14 dogs treated for hydrocephalus by ventriculoperitoneal shunting. *Vet Surg*. 2011;40:183-191.
7. Schmidt MJ, Hartmann A, Farke D, et al. Association between improvement of clinical signs and decrease of ventricular volume after ventriculoperitoneal shunting in dogs with internal hydrocephalus. *J Vet Intern Med*. 2019;33:1368-1375. https://doi.org/10.1111/jvim.15468.
8. Gradner G, Kaefinger R, Dupré G. Complications associated with ventriculoperitoneal shunts in dogs and cats with idiopathic hydrocephalus: a systematic review. *J Vet Intern Med*. 2019;33:403-412. https://doi.org/10.1111/jvim.15422.
9. Pertuiset B, Van Effenterre R, Horn Y. Temporary external valve drainage in hydrocephalus with increased ventricular fluid pressure (experiences with 202 cases). *Acta Neurochir*. 1976;33:173-181. https://doi.org/10.1007/BF01886668.
10. Moringlane JR, von Wild K, Samii M. Clinical value of percutaneous needle trephination (PNT). *Acta Neurochir*. 1980;54:181-189. https://doi.org/10.1007/BF01407084.
11. Hassler W, Zentner J. Ventricle puncture for external CSF drainage and pressure measurement using a modified puncture needle. *Acta Neurochir*. 1988;94:93-95. https://doi.org/10.1007/BF01406623.
12. Aschoff A, Kremer P, Hashemi B, Kunze S. The scientific history of hydrocephalus and its treatment. *Neurosurg Rev*. 1999;22:67-95. https://doi.org/10.1007/s101430050035.
13. Kompanje EJ, Delwel EJ. The first description of a device for repeated external ventricular drainage in the treatment of congenital hydrocephalus, invented in 1744 by Claude-Nicolas Le Cat. *Pediatr Neurosurg*. 2003;39:10-13. https://doi.org/10.1159/000070872.
14. Akinduro OO, Vivas-Buitrago TG, Haranhalli N, et al. Predictors of ventriculoperitoneal shunting following subarachnoid hemorrhage treated with external ventricular drainage. *Neurocrit Care*. 2020;32(3):755-764. https://doi.org/10.1007/s12028-019-00802-8.
15. Mehta A, Mahale R, Khanapure K, Jagannatha AT, Acharya P, Srinivasa R. Acute hydrocephalus in a case of mumps

meningoencephalitis: a rare occurrence. *J Pediatr Neurosci*. 2020;15:34-37. https://doi.org/10.4103/JPN.JPN_58_19.
16. Lee KS, Zhang JJY, Bolem N, et al. Freehand insertion of external ventricular drainage catheter: evaluation of accuracy in a single center. *Asian J Neurosurg*. 2020;15:45-50. https://doi.org/10.4103/ajns.AJNS_292_19.
17. Luong CQ, Nguyen AD, Nguyen CV, et al. Effectiveness of combined external ventricular drainage with intraventricular fibrinolysis for the treatment of intraventricular haemorrhage with acute obstructive hydrocephalus. *Cerebrovasc Dis Extra*. 2019;9:77-89. https://doi.org/10.1159/000501530.
18. Mihalj M, Dolić K, Kolić K, Ledenko V. CSF tap test—obsolete or appropriate test for predicting shunt responsiveness? A systemic review. *J Neurol Sci*. 2016;362:78-84. https://doi.org/10.1016/j.jns.2016.01.028.
19. Abe K, Ono Y, Yoneyama H, et al. Assessment of cerebrospinal fluid flow patterns using the time-spatial labeling inversion pulse technique with 3T MRI: early clinical experiences. *Neuroradiol J*. 2014;27:268-279. https://doi.org/10.15274/NRJ-2014-10045.
20. Yamada S, Miyazaki M, Kanazawa H, et al. Visualization of cerebrospinal fluid movement with spin labeling at MR imaging: preliminary results in normal and pathophysiologic conditions. *Radiology*. 2008;249:644-652. https://doi.org/10.1148/radiol.2492071985.
21. Yamada S, Goto T, McComb JG. Use of a spin-labeled cerebrospinal fluid magnetic resonance imaging technique to demonstrate successful endoscopic fenestration of an enlarging symptomatic cavum septi pellucidi. *World Neurosurg*. 2013a;80:436.e15-18.
22. Yamada S, Miyazaki M, Yamashita Y, et al. Influence of respiration on cerebrospinal fluid movement using magnetic resonance spin labeling. *Fluids Barriers CNS*. 2013;10:36. https://doi.org/10.1186/2045-8118-10-36.
23. Yamada S, Tsuchiya K, Bradley WG, et al. Current and emerging MR imaging techniques for the diagnosis and management of CSF flow disorders: a review of phase-contrast and time-spatial labeling inversion pulse. *Am J Neuroradiol*. 2015;36:623-630. https://doi.org/10.3174/ajnr.A4030.
24. Ito D, Ishikawa C, Jeffery ND, Oshima A, Nakayama T, Kitagawa M. T-SLIP' MRI imaging of cerebrospinal fluid flow through the mesencephalic aqueduct. *J Small Anim Pract*. 2020;61:206-207. https://doi.org/10.1111/jsap.13106.
25. Saito M, Olby NJ, Spaulding K, Munana K, Sharp NJH. Relationship among basilar artery resistance index, degree of ventriculomegaly, and clinical signs in hydrocephalic dogs. *Vet Radiol Ultrasound*. 2003;44:687-694. https://doi.org/10.1111/j.1740-8261.2003.tb00532.x.
26. Bagley RS, Keegan RD, Greene SA, Harrington ML, Moore MP. Pathologic effects in brain after intracranial pressure monitoring in clinically normal dogs, using a fiberoptic monitoring system. *Am J Vet Res*. 1995;56:1475-1478.
27. Di Chiro G. Movement of the cerebrospinal fluid in human beings. *Nature*. 1964;204:290-291. https://doi.org/10.1038/204290a0.
28. Njemanze PC, Beck OJ. MR-gated intracranial CSF dynamics: evaluation of CSF pulsatile flow. *Am J Neuroradiol*. 1989;10:77-80.
29. Yamada S, Kelly E. Cerebrospinal fluid dynamics and the pathophysiology of hydrocephalus: new concepts. *Semin Ultrasound CT MR*. 2016;37:84-91. https://doi.org/10.1053/j.sult.2016.01.001.
30. Thomas WB. Hydrocephalus in dogs and cats. *Vet Clin North Am Small Anim Pract*. 2010;40:143-159. https://doi.org/10.1016/j.cvsm.2009.09.008.
31. Evans HE, de Lahunta A. Miller's anatomy of the dog. In: Fletcher TF, ed. *Spinal Cord and Meninges*. 4th ed. St. Louis, MO: Elsevier; 2013:589-608.
32. Dreha-Kulaczewski S, Joseph AA, Merboldt KD, Ludwig HC, Gärtner J, Frahm J. Identification of the upward movement of human CSF *in vivo* and its relation to the brain venous system. *J Neurosci*. 2017;37:2395-2402. https://doi.org/10.1523/JNEUROSCI.2754-16.2017.
33. Dewey CW. *Encephalopathies*: disorders of the brain. In: Dewey CW, Da Costa RC, eds. *Practical Guide to Canine and Feline Neurology*. 3rd ed. Hoboken, NJ: John Wiley & Sons; 2015:141-236.
34. Scrivani PV, Freer SR, Dewey CW, et al. Cerebrospinal fluid signal-void sign in dogs. *Vet Radiol Ultrasound*. 2009;50:269-275. https://doi.org/10.1111/j.1740-8261.2009.01532.x.
35. Kolecka M, Farke D, Failling K, Kramer M, Schmidt MJ. Intraoperative measurement of intraventricular pressure in dogs with communicating internal hydrocephalus. *PLoS One*. 2019;14:e0222725. https://doi.org/10.1371/journal.pone.0222725.
36. Driver CJ, Volk HA, Rusbridge C, et al. An update on the pathogenesis of syringomyelia secondary to Chiari-like malformations in dogs. *Vet J*. 2013;198:551-559. https://doi.org/10.1016/j.tvjl.2013.07.014.
37. Gardner WJ. Hydrodynamic mechanism of syringomyelia: its relationship to myelocele. *J Neurol Neurosurg Psych*. 1965;28:247-259.
38. Williams B. On the pathologenesis of syringomyelia: a review. *J R Soc Med*. 1980;73:798-806.
39. Sherman JL, Barkovich AJ, Citrin CM. The MR appearance of syringomyelia: new observations. *AJR*. 1987;148:381-391.
40. Dewey CW, Berg JM, Stefanacci JD, Barone G, Marino DJ. Caudal occipital malformation syndrome in dogs. *Compend Contin Educ Pract Vet*. 2004;26:886-896.
41. Rusbridge C, Carruthers H, Dube MP, Holmes M, Jeffery ND. Syringomyelia in cavalier King Charles spaniels: the relationship between syrinx dimensions and pain. *J Small Anim Pract*. 2007;48:423-436.

SUPPORTING INFORMATION

Additional supporting information may be found online in the Supporting Information section at the end of this article.

How to cite this article: Ito D, Ishikawa C, Jeffery ND, Kitagawa M. Cerebrospinal fluid flow on time-spatial labeling inversion pulse images before and after treatment of congenital hydrocephalus in a dog. *J Vet Intern Med*. 2021;35:490–496. https://doi.org/10.1111/jvim.16020

APPENDIX A.

Principle of Time-SLIP sequences

The principle of Time-SLIP sequence is based on the arterial spin-labeling technique. A nonselective inversion-recovery pulse inverts all longitudinal magnetization in the field-of-view. Immediately after the initial inversion, a spatially selective inversion-recovery pulse (tag) returns magnetization of only the fluid and tissue located within the tag region. Therefore, magnetization that originated within the tag will appear bright, whereas magnetization outside of the tag will appear dark. After this preparation, sequential images are repeatedly obtained at differential inversion times, allowing visualizing of CSF displacement. CSF that has traveled outside of the tag during the inversion time will be visualized easily as a bright signal against the dark signal area.